Modeling the quasistatic energy transport between nanoparticles

George Y. Panasyuk* and Kirk L. Yerkes
Aerospace Systems Directorate, Air Force Research Laboratory, Wright-Patterson Air Force Base, Ohio 45433, USA
(Received 16 July 2015; revised manuscript received 1 November 2015; published 22 December 2015)

We consider phononic energy transport between nanoparticles mediated by a quantum particle. The nanoparticles are considered as thermal reservoirs described by ensembles of finite numbers of harmonic oscillators within the Drude-Ullersma model having, in general, unequal mode spacings Δ_1 and Δ_2, which amount to different numbers of atoms in the nanoparticles. The quasistatic energy transport between the nanoparticles on the time scale $t \sim 1/\Delta_{1,2}$ is investigated using the generalized quantum Langevin equation. We find that double degeneracy of system's eigenfrequencies, which occurs in the case of identical nanoparticles, is removed when the mode spacings become unequal. The equations describing the dynamics of the averaged eigenmode energies are derived and solved, and the resulting expression for the energy current between the nanoparticles is obtained and explored. Unlike the case when the thermodynamic limit is assumed resulting in time-independent energy current, finite-size effects result in temporal behavior of the energy current that evinces reversibility features combined with decay and possesses peculiarities at time moments $t = 2\pi n/\Delta_1 + 2\pi m/\Delta_2$ for non-negative integers n and m. When $\Delta_{1,2} \to 0$, an expression for the heat current obtained previously under assumption of the thermodynamic limit is reproduced. The energy current between two platinum nanoparticles mediated by a carbon oxide molecule is considered as an application of the developed model.

DOI: 10.1103/PhysRevE.92.062138 PACS number(s): 05.70.Ln, 05.10.Gg, 65.80.−g

I. INTRODUCTION

Understanding the way how heat transfers through microscopic systems (such as nanowires, nanotubes, molecules, or quantum dots) is one of the most important research directions in modern physics. This study, however, presents many challenges due to nonequilibrium nature of the problem and the necessity to account for quantum properties [1,2]. Also, due to size reduction of electronic devices from the macroscale to nanoscale, a fundamentally new approach to manipulate heat flow becomes increasingly important [3]. Thus, apart from a purely academic interest in the problem, research suggests that nanoscale and molecular systems may be good candidates for many technological advances, such as thermoelectrics [4–7], molecular diodes, switches, rectifiers, and quantum heat transfer in anharmonic junctions [8–11].

There are several approaches to treat heat transport through microscopic systems. One of them is based on the quantum Langevin equation. It was used for studying the thermalization of a particle coupled harmonically to a thermal reservoir and other closely related problems [12–15]. In Refs. [16–19], the approach was used to explore the steady-state heat current and temperature profiles in chains of harmonic oscillators placed between two thermal baths. The closely related "quantum thermal bath method" is also based on the Langevin dynamics [20,21]. It was successfully used for sampling quantum fluctuations within the framework of molecular dynamics (MD) [20] as well as to reproduce the quantum Wigner distribution of a variety of model potentials [21] essentially without any additional computational cost, i.e., without resorting to quantum-mechanical MD [22]. To some extent, a similar approach is developed in Ref. [23], allowing us to avoid direct MD simulation. Based on classical MD, the method employs a coarse-graining procedure that adopts the statistical-operator approach [24] and the classical linear response theory [25]. However, it is based on classical mechanics. The nonequilibrium Green's function (NEGF) method represent another and frequently used approach [26]. It was applied, at first, to calculate electron transport and steady-state properties of a finite system interconnecting reservoirs that are modeled by noninteracting Hamiltonians with infinite degrees of freedom [27–29]. Later, the NEGF approach was applied to phonon transport [30–35]. However, for noninteracting systems, the Langevin approach reproduces the NEGF results exactly [1,36]. In the above-mentioned studies the thermal reservoirs were considered in the thermodynamic limit, i.e., having infinitely large number of modes. Recently, a new method for an exact solution to the Lindblad and Redfield master equations, which can be considered as an alternative to the quantum Langevin equation, has been developed [37–39].

Due to the above-mentioned ongoing miniaturization of electronic devices, size effects, related to finite numbers of atoms in nanosize components of such devices, become increasingly important. For this reason, study of size effects in nanostructured materials occupies an important part of contemporary research. While the study of size and quantum effects in electromagnetic response of nanoparticles have a rather long history (see, for example, Refs. [40–44]), systematic investigation of the role of these effects and their influence on thermal properties of small bodies has taken place only recently. In Refs. [45–47], static thermodynamic properties of nanostructures, such as the local structure of the grain boundary in ultrananocrystals, phonon density of states in nanostructures, and order-disorder transition in nanoparticles, were investigated. In Ref. [48], energy transport in a finite linear harmonic chain was investigated showing the critical role of the on-site pinning potential in establishing a quasi-steady-state condition.

In this paper, we investigate finite-size effects in the case of quasistatic energy transfer between two, not identical in general, nanoparticles mediated by a quantum particle, such

*george.panasyuk.1.ctr@us.af.mil

as a molecule. The nanoparticles and mediator are considered within the harmonic approximation. Our approach is based on the generalized quantum Langevin equation and employs the Drude-Ullersma model for reservoirs' mode spectra. We allow for the mode spacing constants Δ_1 for the first and Δ_2 for the second reservoir to be unequal, which corresponds to different numbers of atoms in the nanoparticles. The dynamics for the average energies of the eigenmodes for the whole system consisting of the nanoparticles and mediator on a time scale $\max(\mathcal{T}_{H1},\mathcal{T}_{H2})$ is described. Here $\mathcal{T}_H \sim \Delta^{-1}$ is the Heisenberg time over which the discreteness of reservoir's energy spectrum becomes resolvable [15,49]. Based on this dynamics, an expression for the energy current between the nanoparticles in the considered time regime is derived and explored.

The paper is organized as follows. The model is introduced in Sec. II, where the generalized Langevin equation is derived and solved and the eigenmodes of the whole system are found and investigated. In Sec. III, equations governing the dynamics of the average energies of the eigenmodes are derived and the expression for the energy current between the reservoirs is obtained. In Sec. IV, the derived equations are approximately solved and the resulting time behavior for the average energies and the energy current is explored. Possible errors associated with the adopted approximations are analyzed. Finally, Sec. V provides brief summary to our research.

II. MODEL

The total Hamiltonian of the system under consideration is similar to that in Refs. [19,50,51]:

$$\mathcal{H}_{\rm tot} = \mathcal{H} + \mathcal{H}_{B1} + \mathcal{H}_{B2} + \mathcal{V}_1 + \mathcal{V}_2. \tag{1}$$

Here

$$\mathcal{H} = \frac{p^2}{2m} + \frac{kx^2}{2} \tag{2}$$

is the Hamiltonian of the quantum particle (the mediator),

$$\mathcal{H}_{B\nu} = \sum_{i=1}^{N_\nu}\left[\frac{p_{\nu i}^2}{2m_{\nu i}} + \frac{m_{\nu i}\omega_{\nu i}^2 x_{\nu i}^2}{2}\right] \tag{3}$$

are the Hamiltonians of the νth thermal reservoir ($\nu = 1, 2$) having N_ν quantum oscillators (modes), and

$$\mathcal{V}_\nu = -x\sum_{i=1}^{N_\nu} C_{\nu i}x_{\nu i} + x^2\sum_{i=1}^{N_\nu}\frac{C_{\nu i}^2}{2m_{\nu i}\omega_{\nu i}^2} \tag{4}$$

describe interaction between the mediator and the reservoirs. In Eq. (2), x and p are the coordinate and momentum operators and m and k are the mass and the spring constant of the central particle. In Eqs. (3) and (4), $x_{\nu i}$ and $p_{\nu i}$ are the coordinate and momentum operators, whereas $m_{\nu i}$ and $\omega_{\nu i}$ are the masses and frequencies of the oscillators for the ith mode that belongs to the νth reservoir. Finally, $C_{\nu i}$ are the coupling coefficients that describe interaction between the particle and reservoirs. The last contributions to the right-hand side of (4) are self-interaction terms, which guarantee that $\mathcal{H}_{B\nu} + \mathcal{V}_\nu$ is positively defined for each ν.

Using solutions of the Heisenberg equations for the reservoirs' operators

$$x_{\nu i}(t) = x_{\nu i}(0)\cos(\omega_{\nu i}t) + \frac{p_{\nu i}(0)}{m_{\nu i}\omega_{\nu i}}\sin(\omega_{\nu i}t) + \frac{C_{\nu i}}{m_{\nu i}\omega_{\nu i}}\int_0^t \sin[\omega_{\nu i}(t-s)]x(s)ds \tag{5}$$

and

$$p_{\nu i}(t) = m_{\nu i}\dot{x}_{\nu i}(t) = -m_{\nu i}\omega_{\nu i}x_{\nu i}(0)\sin(\omega_{\nu i}t) + p_{\nu i}(0)\cos(\omega_{\nu i}t) + C_{\nu i}\int_0^t \cos[\omega_{\nu i}(t-s)]x(s)ds \tag{6}$$

in the Heisenberg equations for x and p, one arrives at the quantum Langevin equation

$$m\ddot{x} = -kx(t) + \eta(t) - \int_0^t \gamma(t-s)\dot{x}(s)ds - \gamma(t)x(0), \tag{7}$$

where

$$\eta(t) = \eta_1(t) + \eta_2(t) \tag{8}$$

is the total noise and

$$\eta_\nu(t) = \sum_{i=1}^{N_\nu} C_{\nu i}\left[x_{\nu i}(0)\cos(\omega_{\nu i}t) + \frac{p_{\nu i}(0)}{m_{\nu i}\omega_{\nu i}}\sin(\omega_{\nu i}t)\right] \tag{9}$$

is the noise coming from the νth reservoir. In the same way,

$$\gamma(t) = \gamma_1(t) + \gamma_2(t) \tag{10}$$

is the friction kernel where

$$\gamma_\nu(t) = \sum_{i=1}^{N_\nu}\frac{C_{\nu i}^2}{m_{\nu i}\omega_{\nu i}^2}\cos(\omega_{\nu i}t) \tag{11}$$

describes interaction of the mediator with the νth reservoir.

The Drude-Ullersma model [14,15,52,53] that we employ here assumes that in the absence of interaction with the central particle, each reservoir consists of uniformly spaced modes and introduces the following frequency dependence for the coupling coefficients:

$$\omega_{\nu i} = i\Delta_\nu, \quad C_{\nu i} = \sqrt{\frac{2\gamma_\nu m_{\nu i}\omega_{\nu i}^2\Delta_\nu D_\nu^2}{\pi\left(\omega_{\nu i}^2 + D_\nu^2\right)}}, \tag{12}$$

where $i = 1,2,\ldots N_\nu$. In Eq. (12), D_ν are the characteristic Debye cutoff frequencies, γ_ν are the coupling constants between a given reservoir and the mediator, and Δ_ν are the mode spacing constants. Unlike that in Ref. [51], we consider Δ_ν as small but finite parameters. Hereafter we assume that

$$D_1 = D_2 \equiv D \text{ and } \gamma_1/m = \gamma_2/m \equiv \gamma/m \equiv \hat{\gamma}, \tag{13}$$

keeping, however, mode spacing constants different. The numbers $N_{1,2}$ of the reservoirs' modes are finite now and we assume that

$$N_\nu = \frac{\omega_{\max}}{\Delta_\nu} \sim \frac{D}{\Delta_\nu}, \quad \nu = 1,2, \tag{14}$$

where $\omega_{\max}$ is the maximum frequency in reservoir's spectrum.

Equation (7) is solved by the Laplace transform [54]:

$$x(t) = \dot{g}(t)x(0) + \frac{1}{m}g(t)p(0) + \frac{1}{m}\int_0^t g(t-s)\eta(s)ds. \tag{15}$$

Here $\dot{g} \equiv dg/dt$,

$$g(t) = L^{-1}\left[\frac{1}{z^2 + w_0^2 + z\hat{\gamma}(z)}\right] = \frac{1}{2\pi i}\int_{c-i\infty}^{c+i\infty}\frac{e^{zt}dz}{h(z)}, \tag{16}$$

where L^{-1} is the inverse of the Laplace transform L, $\omega_0 = \sqrt{k/m}$ is the particle's frequency, and $h(z) = z^2 + w_0^2 + z\hat{\gamma}(z)$. Equations (10), (11), and (12) result in

$$\hat{\gamma}(z) = \frac{1}{m}L[\gamma(t)] = \frac{2\hat{\gamma}D^2 z}{\pi}[\tilde{S}_1(z) + \tilde{S}_2(z)], \tag{17}$$

where

$$\tilde{S}_\nu(z) = \sum_{i=1}^{N_\nu}\frac{\Delta_\nu}{\left(\omega_{\nu i}^2 + D^2\right)\left(\omega_{\nu i}^2 + z^2\right)}. \tag{18}$$

Employing the Heaviside expansion theorem, one obtains

$$g(t) = \sum_n \frac{e^{\tilde{z}_n t}}{h'(\tilde{z}_n)}, \tag{19}$$

where $h'(z) = dh(z)/dz$ and $\tilde{z}_n$ are the roots of $h(z)$. Substitution $\tilde{z}_n = iz_n$ with real z_n transforms the dispersion equation to

$$h(z_n) \equiv \omega_0^2 - z_n^2 + \frac{2\hat{\gamma}D^2 z_n^2}{\pi}[S_1(z_n) + S_2(z_n)] = 0, \tag{20}$$

where

$$S_\nu(z) = -\tilde{S}_\nu(iz). \tag{21}$$

Noticing that $h(-z) = h(z)$, one can rewrite (19) as

$$g(t) = \sum_{n=1}^{N}\frac{\sin z_n t}{z_n \hat{h}(z_n)}, \tag{22}$$

where $N = N_1 + N_2$ and

$$\hat{h}(z) = 1 + \frac{2\hat{\gamma}D^2}{\pi}\sum_{\nu=1}^{2}\sum_{i=1}^{N_\nu}\frac{{\omega_{\nu i}}^2\Delta_\nu}{\left({\omega_{\nu i}}^2 + D^2\right)\left(z^2 - {\omega_{\nu i}}^2\right)}. \tag{23}$$

A simpler case when $\Delta_1 = \Delta_2 \equiv \Delta$ was considered in Ref. [55] where finite sums (21) were approximated by the corresponding series ($N_{1,2} \to \infty$). In that case, the roots of Eq. (20) can be found analytically as an expansion over a small parameter $\tau\Delta$, where

$$\tau \equiv \max\left(\hat{\gamma}^{-1}, \omega_0^{-1}, D^{-1}\right) \ll \Delta^{-1}. \tag{24}$$

As was shown, it is accurate enough to take into account only first two terms in the expansion, so

$$z_n = n\Delta - \psi_n\Delta \tag{25}$$

with

$$\psi_n = \frac{1}{\pi}\arctan\left[\frac{2\hat{\gamma}D^2\omega_n}{\left(\omega_0^2 - \omega_n^2\right)\left(D^2 + \omega_n^2\right) + 2\hat{\gamma}D\omega_n^2}\right]. \tag{26}$$

Here we again assume that Δ_1^{-1} and Δ_2^{-1} are the largest time parameters in the system:

$$\tau \ll \min\left(\Delta_1^{-1}, \Delta_2^{-1}\right). \tag{27}$$

When $\Delta_1 \neq \Delta_2$, we found that the approximation of the finite sums in (20) by the corresponding infinite series can be, at best, only qualitatively correct and we drop this approximation employing correct sums (21) in Eq. (20). It means that an analytical solution for the roots (eigenfrequencies) is no longer available and the roots z_n of (20) are found numerically here. It is interesting to notice, however, that sums

$$Z_\nu(z_n) = \sum_{i=1}^{N_\nu}\frac{{\omega_{\nu i}}^2\Delta_\nu}{\left({\omega_{\nu i}}^2 + D^2\right)\left(z_n^2 - {\omega_{\nu i}}^2\right)^2} \tag{28}$$

in Eq. (23) can be accurately approximated by the corresponding infinite series, so one finds [56]

$$Z_\nu(z_n) \approx \frac{\pi^2}{4\Delta_\nu\left(z_n^2 + D^2\right)\sin^2(\pi z_n/\Delta_\nu)} \tag{29}$$

and

$$\hat{h}(z_n) \approx \frac{\pi\hat{\gamma}D^2}{2}\sum_{\nu=1}^{2}\frac{1}{\Delta_\nu\left(z_n^2 + D^2\right)\sin^2(\pi z_n/\Delta_\nu)}. \tag{30}$$

It happens because the factor $(z^2 - {\omega_{\nu i}}^2)^2$ in the denominator in (23) acts as the "δ function" [unlike just $(z^2 - {\omega_{\nu i}}^2)$ in $S_\nu(z)$]. Our careful analysis shows that approximation (29) produces a relative error of the order of $\mathcal{O}(\tau\Delta_\nu)$ and is small in accordance to (27).

As we found, the total set of the roots z_n, where $n = 1, 2,..., N$, can be split into two subsets: z_{1n} with $n = 1, 2,..., N_1$ and z_{2n} with $n = 1, 2,..., N_2$:

$$\{z_n\}_{n=1}^{N} = \{z_{1n}\}_{n=1}^{N_1}\bigcup\{z_{2n}\}_{n=1}^{N_2}, \quad N = N_1 + N_2. \tag{31}$$

Here the roots z_{1n} from the first subset are obtained iteratively on each interval $[(n-1)\Delta_1,\ n\Delta_1]$ for $n = 1, 2,..., N_1$ starting with $z_{1n}^{(0)} = n\Delta_1$ and the roots z_{2n} from the second one are obtained in the same way on each interval $[(n-1)\Delta_2,\ n\Delta_2]$ for $n = 1, 2,..., N_2$ starting with $z_{2n}^{(0)} = n\Delta_2$. Hence, one can present the roots of the whole system as

$$z_{\nu n} = n\Delta_\nu - \psi_{\nu n}\Delta_\nu, \quad n = 1,2,\ldots,N_\nu, \quad \nu = 1,2, \tag{32}$$

where $\psi_{\nu n}$ are usually relatively small: Our numerical analysis reveals that $\psi_{\nu n} \lesssim 0.1$ for all $z_{\nu n} \leqslant D$ and $\hat{\gamma}/\omega_0 \leqslant 0.1$. Thus, the first and second subsets of the roots are slightly shifted from the sets of the uniformly spaced modes that belong to the first and second thermal reservoir, respectively, before connecting them by the central particle.

If $N_1 = N_2$ (or $\Delta_1 = \Delta_2 \equiv \Delta$), then we have only $N = N_1 = N_2$ different eigenmodes instead of $2N_1$. In this case, each z_n is double degenerate and can be found again by solving Eq. (20). The degeneracy is removed whenever N_2 becomes not equal to N_1, and we return to our general case $\Delta_1 \neq \Delta_2$ when the number of different eigenmodes "jumps" from $N = N_1 = N_2$ to $N = N_1 + N_2$.

III. QUASISTATIC HEAT BALANCE

As one can easily find (see, for example, Ref. [51]), the rate of change of the averaged energy of νth thermal reservoir is

$$\frac{d}{dt}\sum_{i=1}^{N_\nu}\left\langle\frac{p_{\nu i}^2}{2m_{\nu i}}+\frac{m_{\nu i}\omega_{\nu i}^2x_{\nu i}^2}{2}\right\rangle=-\langle\mathcal{P}_\nu\rangle, \tag{33}$$

where the angular brackets denote the ensemble averaging and

$$\langle\mathcal{P}_\nu\rangle=-\sum_{i=1}^{N_\nu}\frac{C_{\nu i}}{2m_{\nu i}}\langle p_{\nu i}x+xp_{\nu i}\rangle \tag{34}$$

is the work done by the νth reservoir on the mediator [16]. Here $x_{\nu i}=x_{\nu i}(t)$, $p_{\nu i}=p_{\nu i}(t)$, and $x=x(t)$ are determined by Eqs. (5), (6), and (15), respectively. These solutions, as well as the resulting balance equation (33) are accurate in frame of the adopted harmonic approximation. Our goal here is to consider only the quasistatic variations of nanoparticles' averaged energies, which happen on a time scale $\max(\Delta_1^{-1},\Delta_2^{-1})\gg\tau$ (27), where we assume that $\Delta_1\sim\Delta_2$. After substitution (6) and (15) into (34), one can drop all terms that are proportional to $g(t)$ or $\dot g(t)$. Indeed, as our numerical analysis shows, $g(t)$ differs noticeably from zero only on time intervals of the order of τ near $t=2\pi n/\Delta_1+2\pi m/\Delta_2$ where $n,m\geqslant 0$ are integers, and we assume [see also the text after Eq. (41)] that these contributions cannot influence nanoparticles's eigenmode average energies. Neglecting the $g(t)$ and $\dot g(t)$ contributions results in the following expression for the energy current:

$$\langle\mathcal{P}_\nu\rangle=J_\nu^{(1)}+J_\nu^{(2)}, \tag{35}$$

where

$$\begin{aligned}J_\nu^{(1)}=-\frac{1}{2m}\sum_{i=1}^{N_\nu}\frac{C_{\nu i}}{m_{\nu i}}\Bigg[&\cos(\omega_{\nu i}t)\int_0^t ds g(t-s)\\&\times\langle p_{\nu i}(0)\eta(s)+\eta(s)p_{\nu i}(0)\rangle-m_{\nu i}\omega_{\nu i}\sin(\omega_{\nu i}t)\\&\times\int_0^t ds g(t-s)\langle x_{\nu i}(0)\eta(s)+\eta(s)x_{\nu i}(0)\rangle\Bigg]\end{aligned} \tag{36}$$

and

$$\begin{aligned}J_\nu^{(2)}=-\frac{1}{2m}\sum_{i=1}^{N_\nu}\frac{C_{\nu i}^2}{m_{\nu i}}\int_0^t ds g(t-s)\\\times\int_0^t d\tau\cos\omega_{\nu i}(t-\tau)\langle x(\tau)\eta(s)+\eta(s)x(\tau)\rangle.\end{aligned} \tag{37}$$

As was shown [15], after coupling of a quantum particle to a thermal reservoir, the whole system comes to equilibrium after the microscopic time τ. Similar to that, in our case of two thermal reservoirs having, in general, different temperatures, the quasistatic energy current will be established during the time τ after connecting the reservoirs by the central particle [55], and our system will consist of set (31) of eigenmodes z_k. Thus, in general, the averaged energy E_ν of the νth reservoir will consist of contributions from all the eigenmodes. On the other hand, it is natural to expect that shortly after connection of the reservoirs, E_ν will be presented mostly by contributions from the νth subset of eigenmodes (32). It will contain also small contributions from the other subset, which we denote as the "ν_1th subset," where $\nu_1=\nu_1(\nu)=1$ if $\nu=2$ and $\nu_1=2$ if $\nu=1$. The latter contributions will grow slowly for $t\geqslant 0$ starting from zero value, because the influence of the central particle on both reservoirs is small, which is reflected in the inequality (27). In addition, we consider here only relatively small coupling constants, when $\hat\gamma/\omega_0\leqslant 0.1$. Thus, one can present E_ν as the sum of the eigenmode average energies

$$E_{\nu k}=\frac{\hbar z_k}{2}n_{\nu k}, \tag{38}$$

where $n_{\nu k}$ is determined by

$$n_{\nu k}=\langle a_k^+a_k+a_ka_k^+\rangle_\nu. \tag{39}$$

In (39), a_k^+ and a_k are the creation and annihilation operators corresponding to the kth eigenmode and satisfying relations

$$\left\langle a_k^+a_{k_1}+a_{k_1}a_k^+\right\rangle_\nu=n_{\nu k}\delta_{k,k_1} \tag{40}$$

and $\langle a_ka_{k_1}\rangle=\langle a_k^+a_{k_1}^+\rangle=0$. The subscript ν in (39) means that, in general, only a (k-dependent) part of the occupation number contributes to $E_{\nu k}$ in (38). Due to the above-mentioned small influence of the mediator on the nanoparticles, one can assume that $n_{\nu k}$ is close to the Bose number

$$\coth(\hbar z_{\nu k}/2k_BT_{\nu k}), \tag{41}$$

if z_k belongs to the νth subset ($z_k=z_{\nu k}$) and $n_{\nu k}$ is very small if z_k belongs to the ν_1th subset ($z_k=z_{\nu_1 k}$) shortly after the connection. Here T_ν are initial temperatures of the nanoparticles. Thus, in accordance to our assumption, supported in Sec. IV, for $t>0$ all the quantities $E_{\nu k}$ and $n_{\nu k}$ vary slowly, changing unnoticeably on the time scale τ starting with the following initial conditions for νth reservoir:

$$E_{\nu k}(0)=\frac{\hbar z_{\nu k}}{2}\coth\frac{\hbar z_{\nu k}}{2k_BT_\nu}, \tag{42}$$

when k belongs to the νth subset, and

$$E_{\nu k}(0)=0, \tag{43}$$

when k belongs to the ν_1th subset. The goal of this section is to derive equations for the eigenmode average energies (38) valid on time scale $t\sim\max(\Delta_1^{-1},\Delta_2^{-1})$.

Using (40), one can find expressions for $\langle x_{\nu i}(0)\eta(s)+\eta(s)x_{\nu i}(0)\rangle$, $\langle p_{\nu i}(0)\eta(s)+\eta(s)p_{\nu i}(0)\rangle$ from (36) and $\langle x(\tau)\eta(s)+\eta(s)x(\tau)\rangle$ from (37) (see Appendix). As is also shown in the Appendix, this results in the following expressions for the two parts of the energy current:

$$\begin{aligned}J_\nu^{(1)}(t)=\frac{2\hbar\hat\gamma^2D^4}{\pi^2}\sum_{k=1}^{N}\frac{n_{\nu k}}{\hat h(z_k)}\\\times\left\{z_k^{-1}S_{\nu k}^{(2)}(t)A_{\nu k}^{(3)}(t)-z_kS_{\nu k}^{(1)}(t)A_{\nu k}^{(2)}(t)\right\}\end{aligned} \tag{44}$$

and

$$\begin{aligned}J_\nu^{(2)}=-\frac{4\hbar\hat\gamma^3D^6}{\pi^3}\sum_{\nu'=1}^{2}\sum_{k=1}^{N}\frac{n_{\nu' k}}{\hat h(z_k)}\\\times\left\{z_k^{-1}S_{\nu' k}^{(2)}(t)W_{\nu\nu' k}^{(2)}(t)+z_kS_{\nu' k}^{(1)}(t)W_{\nu\nu' k}^{(1)}(t)\right\}.\end{aligned} \tag{45}$$

Here

$$A_{\nu k}^{(p)}(t)=-\frac{\partial^p}{\partial t^p}\sum_{i=1}^{N_\nu}\frac{\Delta_\nu\cos\omega_{\nu i}t}{\left(\omega_{\nu i}^2+D^2\right)\left(z_k^2-\omega_{\nu i}^2\right)} \tag{46}$$

for $p = 1, 2$ and $A^{(3)}_{\nu k}(t) = -\partial A^{(2)}_{\nu k}(t)/\partial t$,

$$S^{(p)}_{\nu k}(t) = \int_0^t ds g(s) A^{(p)}_{\nu k}(t-s), \tag{47}$$

and

$$W^{(p)}_{\nu\nu' k}(t) = \sum_{n=1}^{N} \frac{1}{\hat{h}(z_n)} \int_0^t ds A^{(p)}_{\nu' k}(s) \times \left\{ A^{(2)}_{\nu n}(t-s) - A^{(2)}_{\nu n}(0) \cos z_n (t-s) \right\}. \tag{48}$$

Thus, after the time τ, the averaged energy of νth thermal reservoir E_ν becomes the sum of the average energies $E_{\nu k}$ of the eigenmodes and, due to (35), one can write

$$\frac{d}{dt} E_\nu = \sum_{k=1}^{N} \dot{E}_{\nu k} = -\left[J^{(1)}_\nu + J^{(2)}_\nu \right]. \tag{49}$$

Taking into account the structure of expressions (44) and (45), one can rewrite $J^{(1)}_\nu$ and $J^{(2)}_\nu$ in the following form:

$$J^{(1)}_\nu(t) = \sum_{k=1}^{N} j_{\nu k}(t) E_{\nu k} \tag{50}$$

and

$$J^{(2)}_\nu(t) = \sum_{k=1}^{N} [j_{\nu\nu k}(t) E_{\nu k} + j_{\nu\nu_1 k}(t) E_{\nu_1 k}], \tag{51}$$

where $\nu_1 = 1$ if $\nu = 2$ and $\nu_1 = 2$ if $\nu = 1$. Here

$$j_{\nu k}(t) = \frac{2\hat{\gamma}^2 D^4}{\pi^2} \frac{2}{z_k \hat{h}(z_k)} \times \left\{ z_k^{-1} S^{(2)}_{\nu k}(t) A^{(3)}_{\nu k}(t) - z_k S^{(1)}_{\nu k}(t) A^{(2)}_{\nu k}(t) \right\} \tag{52}$$

and

$$j_{\nu\nu_1 k}(t) = -\frac{4\hat{\gamma}^3 D^6}{\pi^3} \frac{2}{z_k \hat{h}(z_k)} \times \left\{ z_k^{-1} S^{(2)}_{\nu_1 k}(t) W^{(2)}_{\nu\nu_1 k}(t) + z_k S^{(1)}_{\nu_1 k}(t) W^{(1)}_{\nu\nu_1 k}(t) \right\}. \tag{53}$$

Now one can represent the energy balance (49) as

$$\sum_{k=1}^{N} \dot{E}_{1k} = -\sum_{k=1}^{N} [(j_{1k} + j_{11k}) E_{1k} + j_{12k} E_{2k}] \tag{54}$$

for the first thermal reservoir and

$$\sum_{k=1}^{N} \dot{E}_{2k} = -\sum_{k=1}^{N} [(j_{2k} + j_{22k}) E_{2k} + j_{21k} E_{1k}] \tag{55}$$

for the second one. Taking into account the energy conservation law for our closed system and neglecting processes of excessive storing and depleting of the energy of the central particle with respect to its average energy during the energy transport, i.e., assuming that we have quasistatic energy transport, one can write that

$$\sum_{k=1}^{N} (\dot{E}_{1k} + \dot{E}_{2k}) = 0. \tag{56}$$

Substituting Eqs. (54) and (55) into (56) and using independence of the eigenmodes, one obtains the following relation:

$$(j_{1k} + j_{11k} + j_{21k}) E_{1k} + (j_{12k} + j_{2k} + j_{22k}) E_{2k} = 0. \tag{57}$$

Noticing that $j_{\nu k}$ and $j_{\nu\nu_1 k}$ do not depend on initial temperatures, we demand that

$$j_{1k} + j_{11k} + j_{21k} = 0 \tag{58}$$

and

$$j_{2k} + j_{22k} + j_{12k} = 0. \tag{59}$$

Using (58) and (59) in Eqs. (54) and (55), one can present the energy balance equations separately for each eigenmode as

$$\dot{E}_{1k} = R_{1k} E_{1k} - R_{2k} E_{2k} \equiv -J_k \tag{60}$$

for the first reservoir and

$$\dot{E}_{2k} = R_{2k} E_{2k} - R_{1k} E_{1k} \equiv J_k \tag{61}$$

for the second one. Here

$$R_{1k} = -[j_{1k}(t) + j_{11k}(t)] \tag{62}$$

and

$$R_{2k} = -[j_{2k}(t) + j_{22k}(t)]. \tag{63}$$

As is clear, Eq. (56) is automatically satisfied by (60) and (61). Coefficients R_{1k} and R_{2k} can be computed based on formulas (52) and (53). Assuming continuity of the eigenmode average energies and taking into account initial conditions (42) and (43), Eqs. (60) and (61) can be solved. After finding $E_{1k}(t)$ and $E_{2k}(t)$, the total energy current $J_{\rm tot}(t)$ can be determined:

$$J_{\rm tot}(t) = \sum_{k=1}^{N} J_k = \sum_{k=1}^{N} [R_{2k} E_{2k}(t) - R_{1k} E_{1k}(t)]. \tag{64}$$

Because there is no work performed by an external force on our isolated system, except for the initial moment, the derived energy current for any $t > 0$ can be interpreted as the heat current.

IV. RESULTS AND DISCUSSION

In order to apply the model described above, we need to choose parameter $\omega_{\max}$ that appears in (14). As was shown in Ref. [55], any values for D and $\omega_{\max}$ that satisfy inequality $D \sim \omega_0 \lesssim \omega_{\max}$ are acceptable and we choose here $\omega_{\max} = 1.3D$. All figures presented below show the corresponding dimensionless quantities.

As follows from our numerical analysis, the coefficients R_{1k} and R_{2k} can be approximated by a sequence of step functions with the steps occur at times

$$t_{nm} = 2\pi n/\Delta_1 + 2\pi m/\Delta_2, \tag{65}$$

where n and m are non-negative integers and it is assumed that times t_{nm} are arranged in an ascending sequence that depends on values of $\Delta_{1,2}$. For example, in the case illustrated in Figs. 1–4, this sequence is $t_{00} = 0 < t_{01} < t_{10} < t_{02} < t_{11} < t_{20} < t_{03}$. In this regard, it is convenient to introduce a single index l in such a way that $\mathcal{T}_l = t_{nm}$, so the above nm sequence corresponds to increasing l from $l = 0$ to $l = 6$.

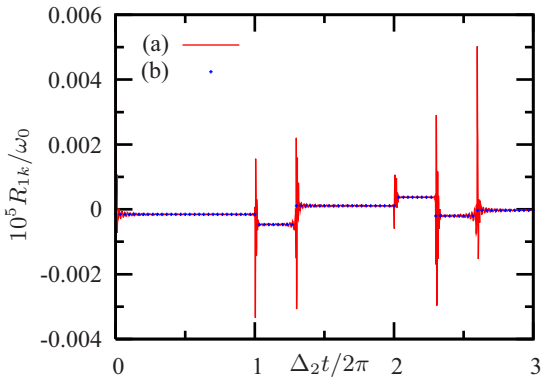

FIG. 1. (Color online) Time dependencies of R_{1k} when $\hat{\gamma}/\omega_0 = 0.1$, $D/\omega_0 = 1$, $\Delta_1/\omega_0 = 0.001$, $\Delta_2/\omega_0 = 0.0013$, and $k = 650$. (a) Accurate result and (b) its approximation by a sequence of step functions determined by Eq. (66).

In accordance to the approximation, $R_{\nu k}(t)$ on a time interval $\mathcal{T}_{l-1} \leqslant t \leqslant \mathcal{T}_l$ is replaced by

$$R_{\nu k}^{(l)} = \frac{1}{\mathcal{T}_l - \mathcal{T}_{l-1}} \int_{\mathcal{T}_{l-1}}^{\mathcal{T}_l} dt\, R_{\nu k}(t) \tag{66}$$

for each ν and k. In Figs. 1–4, we choose $k = 650$ or 651 that correspond to the middle part of nanoparticles' eigenmode spectra. Here $z_{k=651}$ and $z_{k=650}$ belong to the first and second subsets, respectively. As is illustrated in the figures, approximation (66) is correct except for microscopically narrow time intervals $\mathcal{T}_l - \tau < t < \mathcal{T}_l + \tau$ near $\mathcal{T}_l$. One characteristic example of such an interval (near $t = t_{10} = \mathcal{T}_2$) is shown in Fig. 5 for two values of $\hat{\gamma}$. As one finds, the interval where our approximation fails is proportional to $\hat{\gamma}^{-1}$ and is of the order of $\Delta_{1,2}/\hat{\gamma}$ ($\sim$0.01 in the considered case). This failure happens because the energy currents (36) and (37) show transient processes when their time argument passes from one interval $\mathcal{T}_{l-1} < t < \mathcal{T}_l$ to the next one, $\mathcal{T}_l < t < \mathcal{T}_{l+1}$. As was mentioned before, we consider here only the quasistatic regime for the energy transport and neglect these processes. Strictly speaking, we have to exclude these narrow intervals from the time averaging. However, due to relation (27), this exclusion should not change noticeably values of $R_{\nu k}^{(l)}$, which is confirmed by our numerical analysis. The approximation also disregards

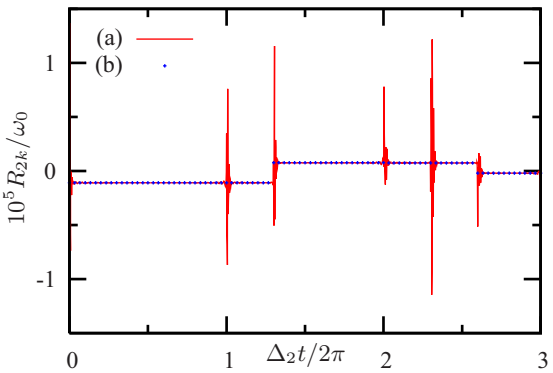

FIG. 2. (Color online) Time dependencies of R_{2k} for the same values of $\hat{\gamma}/\omega_0$, D/ω_0, Δ_1/ω_0, Δ_2/ω_0, and k as in Fig. 1.

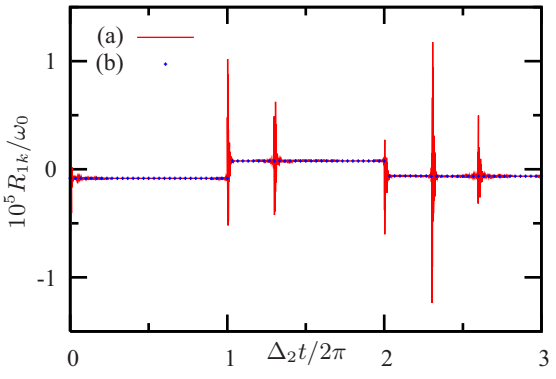

FIG. 3. (Color online) Time dependencies of R_{1k} for the same values of $\hat{\gamma}/\omega_0$, D/ω_0, Δ_1/ω_0, and Δ_2/ω_0 as in Fig. 1, but $k = 651$.

small amplitude "fluctuations" that occur on the time scale τ outside the above-mentioned microscopic time intervals near $\mathcal{T}_l$'s. These small deviations of $R_{\nu k}(t)$ from the corresponding constant values $R_{\nu k}^{(l)}$ may lead to violation of the quasistatic character of the energy current that was assumed in relation (56). In order to estimate the degree of this violation, we consider the ratio

$$\delta = \frac{\left| j_{\nu k}^{(l)} + j_{\nu\nu k}^{(l)} + j_{\nu_1\nu k}^{(l)} \right|}{\max\left(\left| j_{\nu k}^{(l)} \right|, \left| j_{\nu\nu k}^{(l)} \right|, \left| j_{\nu_1\nu k}^{(l)} \right| \right)}, \tag{67}$$

where $j_{\nu k}^{(l)}$ and $j_{\nu_1\nu k}^{(l)}$ are obtained from $j_{\nu k}(t)$ and $j_{\nu_1\nu k}(t)$, respectively, by using them in (66) instead of $R_{\nu k}(t)$. We investigated this ratio for different time intervals $(\mathcal{T}_{l-1}, \mathcal{T}_l)$ and different values of $\Delta_{1,2}$ and found that its characteristic values can be approximately described as $\delta \approx C \times \max(\Delta_1, \Delta_2)/\hat{\gamma}$ with $C \sim 0.1$. Thus, violations of the quasistatic character of the energy current are, indeed, small (and are not clearly seen in Figs. 1–4). It also substantiates Eqs. (58) and (59).

Substituting $R_{\nu k}(t)$ by their averaged values $R_{\nu k}^{(l)}$, one finds $E_{\nu k}(t)$ by solving (60) and (61) with initial conditions (42) and (43) on each time interval $\mathcal{T}_{l-1} < t < \mathcal{T}_l$ and for each k taking into account continuity of $E_{\nu k}(t)$. As an example, Fig. 6 shows temporal behavior of $\delta E_{1k}(t) = E_{1k}(t) - E_{1k}(0)$ for the first nanoparticle for $k = 651$ and 650 that belong to the first and second subsets, respectively. Corresponding time dependence

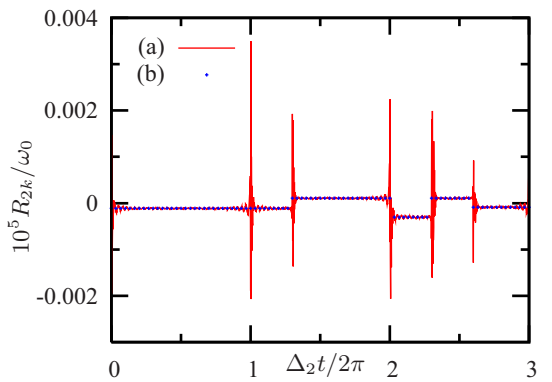

FIG. 4. (Color online) Time dependencies of R_{2k} for the same values of $\hat{\gamma}/\omega_0$, D/ω_0, Δ_1/ω_0, and Δ_2/ω_0 as in Fig. 1 and $k = 651$.

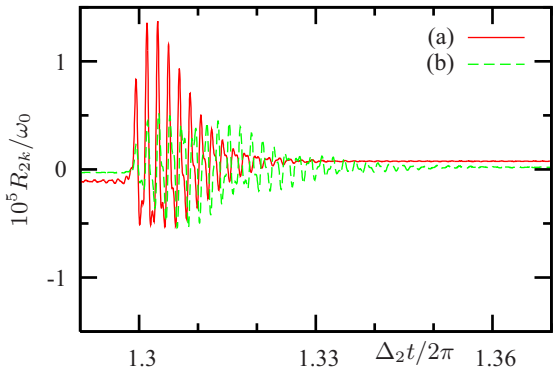

FIG. 5. (Color online) Temporal behavior of R_{2k} when $D/\omega_0 = 1$, $\Delta_1/\omega_0 = 0.001$, $\Delta_2/\omega_0 = 0.0013$, $k = 650$, and (a) $\hat{\gamma}/\omega_0 = 0.1$ and (b) $\hat{\gamma}/\omega_0 = 0.05$.

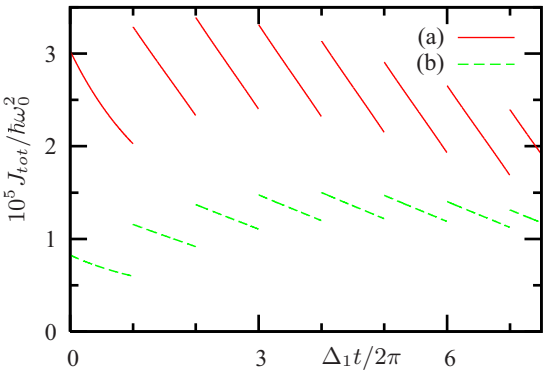

FIG. 7. (Color online) Time dependencies of $J_{\rm tot}$ between identical nanoparticles when $\hat{\gamma}/\omega_0 = 0.1$, $D/\omega_0 = 1$, $\Delta_1/\omega_0 = \Delta_2/\omega_0 = 0.001$, and $\alpha = 0.01$. (a) $k_B\bar{T}/\hbar\omega_0 = 0.2$ and (b) $k_B\bar{T}/\hbar\omega_0 = 0.15$.

of E_{2k} is determined by $E_{2k}(t) = E_{2k}(0) + \delta E_{2k}(t)$, where $\delta E_{2k}(t) = -\delta E_{1k}(t)$, in accordance with Eqs. (60) and (61). The other eigenmode average energies show similar behavior. As one finds, the characteristic time scale over which $E_{\nu k}(t)$ changes noticeably on each interval $(\mathcal{T}_{l-1}, \mathcal{T}_l)$ is of the order of $\Delta_1^{-1} \sim \Delta_2^{-1} \gg \tau$. This observation supports our assumption that the eigenmode average energies change negligibly over τ. Using the obtained solutions for $E_{\nu k}(t)$ in (64), the total energy (or heat) current can be found. Figures 7 and 8 show $J_{\rm tot}(t)$ between identical (Fig. 7) and unequal (Fig. 8) nanoparticles. Because we use approximation (66) that disregards transient processes, all the curves appear discontinuous. We assume that $\alpha \equiv (T_1 - T_2)/\bar{T} \ll 1$. Here $T_{1,2}$ are the initial temperatures of the nanoparticles and $\bar{T}$ is their average. In the case of identical nanoparticles, $R_{2k} = R_{1k} \equiv R_k$ and the expression for the total energy current reduces to

$$J_{\rm tot}(t) = \sum_{k=1}^{N} R_k[E_{2k}(t) - E_{1k}(t)], \tag{68}$$

where the sum is over only $N_1 = N_2 \equiv N$ eigenmodes and their double degeneracy is accounted for by doubling each sum over z_k roots in (22), (44), (45), and (48), and the corresponding changes in (52) and (53). Now the ν_1th subset of the roots z_k, for which initial conditions (43) on $E_{\nu k}(t)$ are imposed, disappears and $E_{\nu k}(0)$ is determined only by (42). After solving (60) and (61), one can find $J_{\rm tot}(t)$ from (68). In the considered case, $J_{\rm tot} \sim \alpha$. Our numerical analysis shows that characteristic values of $J_{\rm tot}(t)$ approach zero when $t \to \infty$. However, these values pass through a maximum which shifts to larger moments of time when $\bar{T}$ decreases, as is illustrated in Fig. 7. As one can notice from the figure, temporal behavior of the energy current appears as quasiperiodic. Similar results were found for the same value of $\hat{\gamma}/\omega_0$ and different Δ in Ref. [57] under approximations described after Eq. (23).

The nature of the temporal behavior of $J_{\rm tot}$ in the case of unequal nanoparticles differs. In both (identical and unequal) cases, we are dealing with energy transport, which is a nonequilibrium process. However, in the case of identical nanoparticles, nonequilibrium is relatively small. It comes from small differences in the average eigenmode energies of the nanoparticles and the energy transport tries to remove these differences. In the case of unequal nanoparticles, nonequilibrium is much stronger, because now partial energy currents J_k coming from νth nanoparticle are proportional to $E_{\nu k}$. They pump energy to the corresponding essentially empty z_k levels of the ν_1th nanoparticle, decreasing $E_{\nu k}$

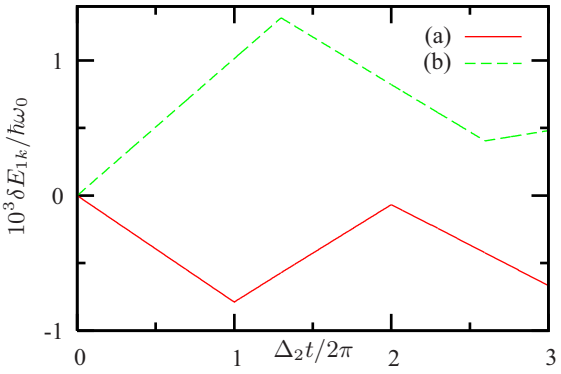

FIG. 6. (Color online) Temporal behavior of δE_{1k} when $\hat{\gamma}/\omega_0 = 0.1$, $D/\omega_0 = 1$, $\Delta_1/\omega_0 = 0.001$, $\Delta_2/\omega_0 = 0.0013$, $k_B\bar{T}/\hbar\omega_0 = 0.1$, and $\alpha = 0.01$. (a) $k = 651$ (first subset) and (b) $k = 650$ (second subset).

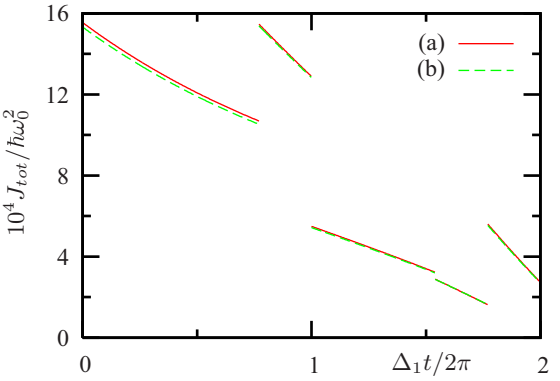

FIG. 8. (Color online) Temporal behavior of $J_{\rm tot}$ between unequal nanoparticles when $\hat{\gamma}/\omega_0 = 0.1$, $D/\omega_0 = 1$, $\Delta_1/\omega_0 = 0.001$, $\Delta_2/\omega_0 = 0.0013$, and $\alpha = 0.01$. (a) $k_B\bar{T}/\hbar\omega_0 = 0.2$ and (b) $k_B\bar{T}/\hbar\omega_0 = 0.1$.

from $E_{\nu k}(0)$. In such a case, J_k depend on $T_{1,2}$ only weakly through $E_{\nu k}(0)$. Because coefficients $R_{\nu k}$ do not depend on $T_{1,2}$, the same kind dependence is expected for $J_{\rm tot}$. This is illustrated in Fig. 8, where $J_{\rm tot}(t)$ only weakly depends on $\bar{T}$. Due to the strong nonequilibrium situation, it would be incorrect, in general, to assume that the resulting average mode energies (or the corresponding occupation numbers) for $t > 0$ are related to the "mode temperatures" in accordance to the Bose formula (as was considered in Ref. [55] for the case of identical nanoparticles), even if the (42) part of the initial conditions assumes so. For this reason, we introduce neither mode temperatures nor average nanoparticle's temperatures and prefer to work only with the average mode energies and energy current. Despite the above-mentioned shifting of the energy levels after interconnecting the nanoparticles, the whole system keeps some resemblance to its properties that existed before the connection. In particular, it still "feels" the difference in periods $2\pi/\Delta_\nu$ of the reservoirs' dynamic variables existed prior to the connection. For this reason, for example, we observe "jumps" of the coefficients R_{1k} and R_{2k} at $t = 2\pi/\Delta_2 < 2\pi/\Delta_1$ that cause the corresponding jump in $J_{\rm tot}(t)$ at the same time moment. As our numerical analysis shows, similar observations are valid for different ratios Δ_1/Δ_2 and different values of $\hat{\gamma}/\omega_0$ and D/ω_0 provided that the inequality (27) is satisfied. It is important to notice, however, that the model becomes inaccurate when $t \gg \max(\Delta_1^{-1}, \Delta_2^{-1})$ for $\Delta_1 \neq \Delta_2$, because for large t it is possible to have $t \approx t_{nm} \approx t_{n_1 m_1}$ with different n,m,n_1, and m_1. In such a case, time interval $|t_{nm} - t_{n_1 m_1}|$ can be small and comparable to τ, violating (27).

Thus, the obtained time dependencies of the energy current demonstrate peculiarities at times t_{nm}. Because this unusual behavior appears due to finite values of $\Delta_{1,2}$, one can expect that the previously derived expressions [51] for $g(t)$ and steady-state current $J_{\rm st}$,

$$g(t) = L^{-1}[\tilde{g}(z)] = \sum_{n=1}^{3} g_n e^{-\mu_n t} \tag{69}$$

and

$$J_{\rm st} = -\frac{\hbar D^2 \hat{\gamma}}{2\pi} \sum_{n=1}^{3} g_n \mu_n^2 \int_0^\infty \frac{d\omega \omega [n_1(\omega) - n_2(\omega)]}{(D^2 + \omega^2)(\mu_n^2 + \omega^2)}, \tag{70}$$

when the thermodynamic limit ($\Delta_{1,2} \to 0$) was assumed from the beginning, can be restored. In Eq. (70), $n_\nu(\omega) = \coth(\hbar\omega/2k_B T_\nu)$ and in (69),

$$\tilde{g}(z) = \frac{D + z}{(D + z)(z^2 + \omega_0^2) + 2D\hat{\gamma} z} = \sum_{n=1}^{3} \frac{g_n}{z + \mu_n}. \tag{71}$$

Here g_n are defined by Eq. (71) and μ_n are the roots of

$$(\mu - D)(\mu^2 + \omega_0^2) + 2\hat{\gamma} D \mu = 0. \tag{72}$$

Indeed, in the considered limit, the adjacent mode levels in both reservoirs become infinitely close, and for any level in the first reservoir the same level can be found in the second one and vice versa. Thus, one can assume that $\Delta_1 = \Delta_2 \equiv \Delta \to 0$. In this case, $N_\nu \to \infty$ and the infinite series in (46) can be calculated accurately [56]:

$$A_{\nu k}^{(p)}(t) = \frac{\pi (z_k)^{p-1}}{2(z_k^2 + D^2) \sin \phi_k} \hat{A}_{\nu k}^{(p)}(t), \tag{73}$$

where $\hat{A}_{\nu k}^{(1)}(t) = \hat{A}_{\nu k}^{(3)}(t) = \sin(z_k t - \phi_k)$, $\hat{A}_{\nu k}^{(2)}(t) = \cos(z_k t - \phi_k)$, and $\phi_k = \pi z_k/\Delta$. If $\Delta_1 = \Delta_2 \equiv \Delta$, analytical solution (25) and (26) can be used and one finds [55]

$$g(t) = -\frac{i}{\pi} \sum_{n=1}^{3} g_n \sum_{k=-\infty}^{\infty} \frac{\Delta z_k e^{i z_k t}}{z_k^2 + \mu_n^2}. \tag{74}$$

When $\Delta \to 0$, the sum over k transforms into the integral. Closing the integration contour in the upper complex half-plane (for $t > 0$), one arrives at (69). Using (69) in (47) with $A_{\nu k}^{(p)}(t)$ determined from (73), one finds that

$$z_k^{-1} S_{\nu k}^{(2)} A_{\nu k}^{(3)} - z_k S_{\nu k}^{(1)} A_{\nu k}^{(2)} = \frac{\pi^2 z_k^3}{4(z_k^2 + D^2)^2 \sin^2 \phi_k} \sum_{n=1}^{3} \frac{g_n}{\mu_n^2 + z_k^2} \tag{75}$$

and does not depend on time. Substituting (30) with $\Delta_1 = \Delta_2 = \Delta$ and (75) into (44), one reduces $J_\nu^{(1)}$ to

$$J_\nu^{(1)} = \frac{\hbar \hat{\gamma} D^2}{\pi} \sum_{n=1}^{3} g_n \sum_{k=1}^{N} \frac{\Delta z_k^3 n_\nu(z_k)}{(z_k^2 + D^2)(\mu_n^2 + z_k^2)}. \tag{76}$$

Using (69) and (73), $J_\nu^{(2)}$ can be obtained in the same way. However, one can use $J_{\rm tot}$ in a simpler equivalent form

$$J_{\rm tot} = \tfrac{1}{2}\left[J_1^{(1)} - J_2^{(1)}\right] \tag{77}$$

due to canceling $J_{1,2}^{(2)}$ contributions when $\Delta_1 = \Delta_2$. After substituting (76) into (77) and converting the sum into the integral, one can extend its upper limit to infinity, taking into account fast (exponential) convergence of the integral. Due to (22), $g(0) = g_1 + g_2 + g_3 = 0$ and $J_{\rm tot}$ reduces to $J_{\rm st}$.

Finally, we briefly consider an application of our model to study phononic heat transport between two platinum nanoparticles interconnected by a carbon oxide (CO) molecule. In order to determine the heat current in this case, we take into account experimental value $\omega_0 = 480\ {\rm cm}^{-1}$, corresponding to the central frequency of Pt-C stretching vibration bond [58]. In order to estimate $\hat{\gamma}/\omega_0$, we observe that the FWHM of the Pt-C vibration mode is approximately $60\ {\rm cm}^{-1}$ [58], which amounts to $\hat{\gamma}/\omega_0 \approx 0.13$. We choose $T_1 = 70$ K, which corresponds to $k_B \bar{T}/\hbar\omega_0 = 0.1$ for $\alpha = 0.01$. Taking into account that the platinum Debye frequency is $D \approx 0.021\, eV/\hbar$, we have $D/\omega_0 = 0.35$. In order to make the result comparable to the one shown in Fig. 8, we assume that the numbers of Pt atoms in the nanoparticles, $N_{\rm at1}$ and $N_{\rm at2}$, are such that the corresponding mode spacings are the same as in Fig. 8, i.e., $\Delta_1/\omega_0 = 0.001$ and $\Delta_2/\omega_0 = 0.0013$. The resulting temporal dependence for $J_{\rm tot}$ in accordance to our prediction is shown in Fig. 9. It is qualitatively similar to the one in Fig. 8; however, the characteristic values of the heat current are smaller, despite the fact that $\hat{\gamma}/\omega_0$ in Fig. 9 is larger. This is because D/ω_0 in the latter case is smaller, decreasing the resulting effective reservoir-particle interaction strength and, hence, the heat current [51].

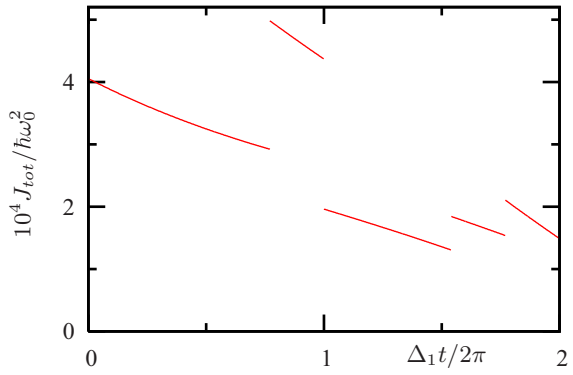

FIG. 9. (Color online) Time dependencies of $J_{\rm tot}$ between Pt nanoparticles when $\hat{\gamma}/\omega_0 = 0.13$, $D/\omega_0 = 0.35$, $\Delta_1/\omega_0 = 0.001$, $\Delta_2/\omega_0 = 0.0013$, $k_B\bar{T}/\hbar\omega_0 = 0.1$, and $\alpha = 0.01$.

V. CONCLUSIONS

We have considered finite-size effects in the energy (heat) transport between two nanoparticles mediated by a quantum particle, such as a molecule or an atomic chain. The nanoparticles have, in general, different numbers of atoms resulting in different mode spacings $\Delta_1 \neq \Delta_2$. They are represented as thermal reservoirs described by ensembles of oscillators using the generalized quantum Langevin equation combined with the Drude-Ullersma model. We have derived and numerically solved the dispersion equation describing the eigenmodes of our system. As is shown, the double degeneracy of the eigenmodes that exists for the case of identical nanoparticles, when $\Delta_1 = \Delta_2$, is removed if $\Delta_1 \neq \Delta_2$. Equations that govern temporal behavior of the average energies of system's eigenmodes are derived and approximately solved. An expression that describes the time evolution of the heat current $J_{\rm tot}$ between the nanoparticles is found and explored. In addition, we analyzed the obtained results for possible errors and violations of the quasistatic regime and found that they are small and can be neglected. As revealed, the time evolution of all the considered quantities demonstrates peculiarities at time moments $t = 2\pi n/\Delta_1 + 2\pi m/\Delta_2$ for non-negative integers n and m. For the case of identical nanoparticles, these peculiarities can be delineated as quasiperiodicity. In this case, the total heat current is proportional to the difference of initial nanoparticles' temperatures $T_{1,2}$. Degeneracy removal modifies the temporal behavior of the heat current due to stronger nonequilibrium nature of the dynamics, making it less sensitive to variations of $T_{1,2}$. In both cases, the appeared peculiarities are due to discreteness of nanoparticles' energy spectra and represent finite-size effects. As is shown, in the thermodynamic limit, when $\Delta_{1,2} \to 0$, the produced expression for the heat current reduces to the one obtained previously [51]. Finally, the heat current between platinum nanoparticles mediated by a CO molecule is considered as an example of application of the developed model.

ACKNOWLEDGMENTS

The authors acknowledge that this research was funded by the United States Air Force Office of Scientific Research.

APPENDIX

The dynamics of $x_{\nu i}$ and $p_{\nu i}$ is determined by [15,55]

$$x_{\nu i}(t) = \sum_k \sqrt{\frac{\hbar}{2m_{\nu i} z_k}}\, e^k_{\nu i}\left(a_k^+ e^{iz_k t} + a_k e^{-iz_k t}\right) \tag{A1}$$

and $p_{\nu i}(t) = m_{\nu i}\dot{x}_{\nu i}(t)$, where $\{e^k\}$ are orthonormal eigenvectors that diagonalize the Hamiltonian (1) and correspond to the eigenfrequencies z_k:

$$e^k_{\nu i} = \sqrt{\frac{2\hat{\gamma}\Delta_\nu}{\pi\hat{h}(z_k)\left(\omega_{\nu i}^2 + D^2\right)}}\,\frac{\omega_{\nu i} D}{\omega_{\nu i}^2 - z_k^2}, \quad \nu = 1,2. \tag{A2}$$

Here $\hat{h}(z_k)$ is determined by (23). Employing (A1), $p_{\nu i}(t) = m_{\nu i}\dot{x}_{\nu i}(t)$, (40), and taking into account the assumption discussed after Eq. (40), one finds for νth reservoir

$$\langle x_{\nu i}(0)x_{\nu j}(0) + x_{\nu j}(0)x_{\nu i}(0)\rangle = \frac{\hbar}{\sqrt{m_{\nu i}m_{\nu j}}}\sum_{k=1}^N \frac{n_{\nu k} e^k_{\nu i} e^k_{\nu j}}{z_k}, \tag{A3}$$

$$\langle p_{\nu i}(0)p_{\nu j}(0) + p_{\nu j}(0)p_{\nu i}(0)\rangle = \hbar\sqrt{m_{\nu i}m_{\nu j}}\sum_{k=1}^N n_{\nu k} e^k_{\nu i} e^k_{\nu j} z_k, \tag{A4}$$

and

$$\langle x_{\nu i}(0)p_{\nu i}(0) + p_{\nu i}(0)x_{\nu i}(0)\rangle = 0. \tag{A5}$$

Thus, the ensemble averages in (36) are

$$\langle x_{\nu i}(0)\eta(s) + \eta(s)x_{\nu i}(0)\rangle = \sqrt{\frac{m}{m_{\nu i}}}\,\bar{A}_{\nu i}\sum_{k=1}^N \frac{n_{\nu k} A^{(2)}_{\nu k}(s)}{\hat{h}(z_k) z_k\left(z_k^2 - \omega_{\nu i}^2\right)} \tag{A6}$$

and

$$\langle p_{\nu i}(0)\eta(s) + \eta(s)p_{\nu i}(0)\rangle = \sqrt{m m_{\nu i}}\,\bar{A}_{\nu i}\sum_{k=1}^N \frac{n_{\nu k} z_k A^{(1)}_{\nu k}(s)}{\hat{h}(z_k)\left(z_k^2 - \omega_{\nu i}^2\right)}. \tag{A7}$$

In these relations,

$$\bar{A}_{\nu i} = \frac{2\hbar\hat{\gamma} D^3\omega_{\nu i}}{\pi}\sqrt{\frac{2\hat{\gamma}\Delta_\nu}{\pi\left(\omega_{\nu i}^2 + D^2\right)}} \tag{A8}$$

and $A^{(p)}_{\nu k}(t)$ is defined in (46). Substituting (A6) and (A7) in Eq. (36), one finds

$$J^{(1)}_\nu(t) = \sum_{k=1}^N \frac{n_{\nu k}}{z_k\hat{h}(z_k)}\int_0^t ds g(t-s)A^{(2)}_{\nu k}(s) \times \sum_{i=1}^{N_\nu}\frac{C_{\nu i}\bar{A}_{\nu i}\omega_{\nu i}\sin\omega_{\nu i}t}{2\sqrt{m m_{\nu i}}\left(z_k^2 - \omega_{\nu i}^2\right)}$$

$$-\sum_{k=1}^{N}\frac{n_{\nu k}z_k}{\hat{h}(z_k)}\int_0^t ds g(t-s)A_{\nu k}^{(1)}(s)$$
$$\times\sum_{i=1}^{N_\nu}\frac{C_{\nu i}\bar{A}_{\nu i}\cos\omega_{\nu i}t}{2\sqrt{mm_{\nu i}}\left(z_k^2-\omega_{\nu i}^2\right)}. \quad \text{(A9)}$$

The use of (A8) and (46) in Eq. (A9) results in (44).

In order to reduce the expression for $J_\nu^{(2)}$, we substitute solution (15) for the Langevin equation into Eq. (37). After dropping the terms that contain $g(t)$ or $\dot{g}(t)$, one obtains

$$\langle x(t)\eta(s)+\eta(s)x(t)\rangle = \frac{1}{m}\int_0^t d\tau g(t-\tau)\langle\eta(\tau)\eta(s)+\eta(s)\eta(\tau)\rangle. \quad \text{(A10)}$$

Using (8), (9), (A3)–(A5), and (46), one finds that

$$\frac{1}{m}\langle\eta(\tau)\eta(s)+\eta(s)\eta(\tau)\rangle = \frac{4\hbar\hat{\gamma}^2D^4}{\pi^2}\sum_{\nu=1}^{2}\sum_{k=1}^{N}\frac{n_{\nu k}}{\hat{h}(z_k)} \times\left\{z_k^{-1}A_{\nu k}^{(2)}(\tau)A_{\nu k}^{(2)}(s)+z_kA_{\nu k}^{(1)}(\tau)A_{\nu k}^{(1)}(s)\right\}. \quad \text{(A11)}$$

Substituting (A11) back into (A10) and using (47) results in

$$\langle x(t)\eta(s)+\eta(s)x(t)\rangle = \frac{4\hbar\hat{\gamma}^2D^4}{\pi^2}\sum_{\nu=1}^{2}\sum_{k=1}^{N}\frac{n_{\nu k}}{\hat{h}(z_k)} \times\left\{z_k^{-1}S_{\nu k}^{(2)}(t)A_{\nu k}^{(2)}(s)+z_kS_{\nu k}^{(1)}(t)A_{\nu k}^{(1)}(s)\right\}. \quad \text{(A12)}$$

Finally, using (A12) and (12) in Eq. (37), one can write

$$J_\nu^{(2)} = -\frac{4\hbar\hat{\gamma}^3D^6}{\pi^3}\sum_{\nu'=1}^{2}\sum_{k=1}^{N}\frac{n_{\nu' k}}{\hat{h}(z_k)} \times\left\{z_k^{-1}S_{\nu' k}^{(2)}(t)W_{\nu\nu' k}^{(2)}(t)+z_kS_{\nu' k}^{(1)}(t)W_{\nu\nu' k}^{(1)}(t)\right\}. \quad \text{(A13)}$$

Here $W_{\nu\nu' k}^{(p)}(t)$ is defined as

$$W_{\nu\nu' k}^{(p)}(t) = \sum_{i=1}^{N_\nu}\frac{\Delta_\nu\omega_{\nu i}^2}{\omega_{\nu i}^2+D^2}\int_0^t ds\cos\omega_{\nu i}(t-s)S_{\nu' k}^{(p)}(s).$$

Using Eqs. (22), (46) , and (47), one reduces $W_{\nu\nu' k}^{(p)}$ to (48).

[1] A. Dhar, Adv. Phys. **57**, 457 (2008).
[2] Y. Dubi and M. Di Ventra, Rev. Mod. Phys. **83**, 131 (2011).
[3] G. Cerefolini, *Nanoscale Devices* (Springer, Berlin, 2009).
[4] A. I. Hochbaum *et al.*, Nature (London) **451**, 163 (2008).
[5] A. I. Boukai *et al.*, Nature (London) **451**, 168 (2008).
[6] M. Galperin, M. A. Ratner, and A. Nitzan, J. Phys. Condens. Matter **19**, 103201 (2007).
[7] C. A. Perroni, D. Ninno, and V. Cataudella, Phys. Rev. B **90**, 125421 (2014).
[8] *Molecular Electronics*, edited by J. Jortner and M. Ratner (Blackwell Science, Oxford, 1997).
[9] P. Hänggi, M. Ratner, and S. Yalikari, Chem. Phys. **281**, 111 (2002).
[10] D. Segal, Phys. Rev. Lett. **100**, 105901 (2008).
[11] D. Segal, Phys. Rev. E **90**, 012148 (2014).
[12] A. O. Caldeira and A. J. Leggett, Physica **121**, 587 (1983).
[13] Y. L. Klimontovich, *Statistical Theory of Open Systems* (Kluwer, Amsterdam, 1997).
[14] A. E. Allahverdyan and Th. M. Nieuwenhuizen, Phys. Rev. Lett. **85**, 1799 (2000).
[15] Th. M. Nieuwenhuizen and A. E. Allahverdyan, Phys. Rev. E **66**, 036102 (2002).
[16] U. Zürcher and P. Talkner, Phys. Rev. A **42**, 3278 (1990).
[17] K. Saito, S. Takesue, and S. Miyashita, Phys. Rev. E **61**, 2397 (2000).
[18] A. Dhar and B. S. Shastry, Phys. Rev. B **67**, 195405 (2003).
[19] D. Segal, A. Nitzan, and P. Hänggi, J. Chem. Phys **119**, 6840 (2003).
[20] H. Dammak, Y. Chalopin, M. Laroche, M. Hayoun, and J.-J. Greffet, Phys. Rev. Lett. **103**, 190601 (2009).
[21] M. Basire, D. Borgis, and R. Vuilleumier, Phys. Chem. Chem. Phys. **15**, 12591 (2013).
[22] R. Car and M. Parrinello, Phys. Rev. Lett. **55**, 2471 (1985).
[23] X. Li, Phys. Rev. E **90**, 032112 (2014).
[24] D. N. Zubarev, Fortschr. Phys. **18**, 125 (1970).
[25] M. Toda, R. Kubo, and N. Hashitsume, *Statistical Physics II: Nonequilibrium Statistical Mechanics* (Springer, Berlin, 1983).
[26] L. V. Keldysh, Sov. Phys. JETP **20**(4), 1018 (1965).
[27] C. Caroli, R. Combescot, P. Nozieres, and D. Saint-James, J. Phys. C **4**, 916 (1971).
[28] Y. Meir and N. S. Wingreen, Phys. Rev. Lett. **68**, 2512 (1992).
[29] S. Datta, *Electronic Transport in Mesoscopic Systems* (Cambridge University Press, Cambridge, 1995).
[30] A. Ozpineci and S. Ciraci, Phys. Rev. B **63**, 125415 (2001).
[31] T. Yamamoto and K. Watanabe, Phys. Rev. Lett. **96**, 255503 (2006).
[32] J. S. Wang, N. Zeng, J. Wang, and C. K. Gan, Phys. Rev. E **75**, 061128 (2007).
[33] T. Ojanen and A. P. Jauho, Phys. Rev. Lett. **100**, 155902 (2008).
[34] A. Dhar and D. Roy, J. Stat. Phys. **125**, 801 (2006).
[35] K. Walczak and K. L. Yerkes, J. Appl. Phys. **115**, 174308 (2014).
[36] J. S. Wang, J. Wang, and J. T. Lü, Eur. Phys. J. B **62**, 381 (2008).
[37] T. Prosen, New J. Phys. **10**, 043026 (2008).
[38] T. Prosen and B. Žunkovič, New J. Phys. **12**, 025016 (2010).
[39] J. Thinga, J. S. Wang, and P. Hänggi, J. Chem. Phys. **136**, 194110 (2012).
[40] F. Hache, D. Ricard, and C. Flytzanis, J. Opt. Soc. Am. B **3**, 1647 (1986).
[41] S. G. Rautian, Sov. Phys. JETP **85**, 451 (1997).
[42] G. Y. Panasyuk, J. C. Schotland, and V. A. Markel, Phys. Rev. Lett. **100**, 047402 (2008).
[43] A. A. Govyadinov, G. Y. Panasyuk, J. C. Schotland, and V. A. Markel, Phys. Rev. B **84**, 155461 (2011).
[44] G. Y. Panasyuk, J. C. Schotland, and V. A. Markel, Phys. Rev. B **84**, 155460 (2011).

[45] S. P. Adiga, V. P. Adiga, R. W. Carpick, and D. W. Brenner, J. Phys. Chem. C **115**, 21691 (2011).
[46] D. Sopu, J. Kotakoski, and K. Albe, Phys. Rev. B **83**, 245416 (2011).
[47] J. Pohl, C. Stahl, and K. Albe, Beilstein J. Nanotechnol. **3**, 1 (2012).
[48] E. C. Cuansing, H. Li, and J. S. Wang, Phys. Rev. E **86**, 031132 (2012).
[49] F. Haake, *Quantum Signatures of Chaos* (Springer, Berlin, 2001).
[50] G. W. Ford, J. T. Lewis, and R. F. O'Connell, Phys. Rev. A **37**, 4419 (1988).
[51] G. Y. Panasyuk, G. A. Levin, and K. L. Yerkes, Phys. Rev. E **86**, 021116 (2012).
[52] P. Ullersma, Physica (Utrecht) **32**, 27 (1966); **32**, 56 (1966); **32**, 74 (1966); **32**, 90 (1966).
[53] U. Weiss, *Quantum Dissipative Systems* (World Scientific, Singapore, 1993).
[54] R. V. Churchill, *Operational Mathematics*, 2nd ed. (McGraw-Hill, New York, 1972).
[55] G. Y. Panasyuk and K. L. Yerkes, Phys. Rev. E **87**, 062118 (2013).
[56] A. P. Prudnikov, Y. A. Brychkov, and O. I. Marichev, *Integrals and Series: Elementary Functions*, Vol. 1 (Gordon and Breach, Amsterdam, 1998).
[57] G. Y. Panasyuk, T. J. Haugan, and K. L. Yerkes, MRS Proc. **1704** (2014).
[58] G. Blyholder and R. Sheets, J. Phys. Chem. **74**, 4335 (1970).